

**$B^0 \rightarrow \omega\eta^{(\prime)}$  and  $\phi\eta^{(\prime)}$  decays in the perturbative QCD approach**Dong-qin Guo,<sup>\*</sup> Xin-fen Chen,<sup>†</sup> and Zhen-jun Xiao<sup>‡</sup>*Department of Physics and Institute of Theoretical Physics, Nanjing Normal University, Nanjing, Jiangsu 210097, People's Republic of China*

(Received 12 February 2007; published 30 March 2007)

We calculate the branching ratios and  $CP$ -violating asymmetries for  $B^0 \rightarrow \omega\eta$ ,  $\omega\eta'$ ,  $\phi\eta$ , and  $\phi\eta'$  decays in the perturbative QCD (pQCD) factorization approach. The pQCD predictions for the  $CP$ -averaged branching ratios are  $\text{Br}(B^0 \rightarrow \omega\eta) = (2.7_{-1.1}^{+1.1}) \times 10^{-7}$ ,  $\text{Br}(B^0 \rightarrow \omega\eta') = (0.75_{-0.33}^{+0.37}) \times 10^{-7}$ , and  $\text{Br}(B^0 \rightarrow \phi\eta) = (6.3_{-1.9}^{+3.3}) \times 10^{-9}$ ,  $\text{Br}(B^0 \rightarrow \phi\eta') = (7.3_{-2.6}^{+3.5}) \times 10^{-9}$  which are consistent with currently available experimental upper limits. The inclusion of the gluonic contribution can change the branching ratios of  $B \rightarrow \omega(\phi)\eta'$  decays by about 10%. The direct  $CP$ -violating asymmetries for  $B^0 \rightarrow \omega\eta$  and  $\omega\eta'$  decays are generally large in size.

DOI: [10.1103/PhysRevD.75.054033](https://doi.org/10.1103/PhysRevD.75.054033)

PACS numbers: 13.25.Hw, 12.38.Bx, 14.40.Nd

**I. INTRODUCTION**

As is well known, the two-body charmless  $B$  meson decays provide a good place for testing the standard model (SM) and searching for the new physics signals. Among various  $B \rightarrow M_1 M_2$  (here  $M_i$  refers to the light pseudoscalar or vector mesons) decay channels, the decays involving the  $\eta$  or  $\eta'$  meson in the final state have been studied extensively during the past decade because of the so-called  $K\eta'$  puzzle or other special features.

In Ref. [1], for example, many decay modes involving  $\eta^{(\prime)}$  meson were studied in the QCD factorization (QCDF) approach [2]. In the pQCD factorization approach [3], on the other hand, the  $B \rightarrow K\eta^{(\prime)}$ ,  $\rho\eta^{(\prime)}$ ,  $\pi\eta^{(\prime)}$ , and  $\eta^{(\prime)}\eta^{(\prime)}$  decays have been calculated in Refs. [4–7]. The  $B_s \rightarrow (\pi, \rho, \omega, \phi)\eta^{(\prime)}$  decays, furthermore, have also been studied in the pQCD approach [8].

In this paper, we will perform the leading order pQCD calculation for  $B \rightarrow \omega\eta^{(\prime)}$  and  $\phi\eta^{(\prime)}$  decays. Besides the usual factorizable contributions, we here are able to evaluate the nonfactorizable and the annihilation contributions as well. Besides the dominant contributions from the  $q\bar{q}$  components of  $\eta^{(\prime)}$  mesons, the contribution from the possible gluonic component of the  $\eta^{(\prime)}$  meson will also be included by using the formulae as given in Ref. [9].

On the experimental side, only the upper limits on the branching ratios of  $B \rightarrow \omega(\phi)\eta^{(\prime)}$  decays are available now [10,11]

$$\begin{aligned} \text{Br}(B^0 \rightarrow \phi\eta) &< 0.6 \times 10^{-6}, \\ \text{Br}(B^0 \rightarrow \phi\eta') &< 1.0 \times 10^{-6}. \end{aligned} \quad (1)$$

$$\begin{aligned} \text{Br}(B^0 \rightarrow \omega\eta) &< 1.9 \times 10^{-6}, \\ \text{Br}(B^0 \rightarrow \omega\eta') &< 2.8 \times 10^{-6}. \end{aligned} \quad (2)$$

But these decays could be measured with good precision in the forthcoming LHC-b experiments if their decay rates are larger than  $10^{-8}$ .

For  $B \rightarrow \omega(\phi)\eta^{(\prime)}$  decays considered here, it is generally believed that the  $q\bar{q}$  component of the  $\eta^{(\prime)}$  meson provide the dominant contribution, but it is still very difficult to calculate reliably the gluonic contribution from the possible gluonic component of the  $\eta^{(\prime)}$  meson [9,12]. Of course, great efforts have been made for this problem and some progress has been achieved recently [9,12] in order to explain the large  $B \rightarrow K\eta'$  decay rates. In Ref. [9], for instance, the authors found that the possible gluonic contribution is small for both  $B \rightarrow \eta$  and  $B \rightarrow \eta'$  form factors [9,13].

This paper is organized as follows. In Sec. II, we give a brief review for the pQCD factorization approach. In Sec. III, we calculate analytically the related Feynman diagrams and present the various decay amplitudes for the studied decay modes. In Sec. IV, we show the numerical results for the branching ratios and  $CP$  asymmetries of  $B \rightarrow \omega(\phi)\eta^{(\prime)}$  decays. The summary and some discussions are included in the final section.

**II. THE THEORETICAL FRAMEWORK**

At the present, there exist two popular factorization approaches to calculate the hadronic matrix element  $\langle M_1 M_2 | O_i | B \rangle$ : the QCDF approach [2] and the pQCD approach [3,14,15]. The pQCD approach has been developed earlier from the QCD hard-scattering approach [15]. Some elements of this approach are also present in the QCD factorization approach [1,2]. The two major differences between these two approaches are (a) the form

<sup>\*</sup>Electronic address: medongqin@163.com<sup>†</sup>Electronic address: chenxinfen@163.com<sup>‡</sup>Electronic address: xiaozhenjun@njnu.edu.cn

factors are calculable perturbatively in pQCD approach, but taken as the input parameters extracted from other experimental measurements in the QCDF approach; and (b) the annihilation contributions are calculable and play an important role in producing  $CP$  violation for the considered decay modes in pQCD approach, but it could not be evaluated reliably in QCDF approach. Of course, the assumptions behind the pQCD approach, specifically the possibility to calculate the form factors perturbatively, are still under discussion [16]. More efforts are needed to clarify these problems.

In pQCD approach, the decay amplitude is separated into soft ( $\Phi$ ), hard ( $H$ ), and harder ( $C$ ) dynamics characterized by different energy scales ( $t, m_b, M_W$ ). It is conceptually written as the convolution

$$\begin{aligned} \mathcal{A}(B \rightarrow M_1 M_2) \sim & \int d^4 k_1 d^4 k_2 d^4 k_3 \\ & \times \text{Tr}[C(t)\Phi_B(k_1)\Phi_{M_1}(k_2)\Phi_{M_2}(k_3) \\ & \times H(k_1, k_2, k_3, t)], \end{aligned} \quad (3)$$

where the  $k_i$  are the momenta of the light quarks included in each of the mesons, and Tr denotes the trace over Dirac and color indices.  $C(t)$  is the Wilson coefficient which results from the radiative corrections at short distance. In the above convolution,  $C(t)$  includes the harder dynamics at larger scale than  $M_B$  scale and describes the evolution of local 4-Fermi operators from  $m_W$  (the  $W$  boson mass) down to the  $t \sim \mathcal{O}(\sqrt{\bar{\Lambda}M_B})$  scale, where  $\bar{\Lambda} \equiv M_B - m_b$ . The function  $H(k_1, k_2, k_3, t)$  is the hard part and can be calculated perturbatively. The function  $\Phi_M$  is the wave function which describes hadronization of the quark and antiquark to the meson  $M$ . While the function  $H$  depends

on the process considered, the wave function  $\Phi_M$  is independent of the specific decay process. Using the wave functions determined from other well-measured processes, one can make quantitative predictions here.

Since the  $b$  quark is rather heavy, we consider the  $B$  meson at rest for simplicity. It is convenient to use the light cone coordinate  $(p^+, p^-, \mathbf{p}_T)$  to describe the meson's momenta,

$$p^\pm = \frac{1}{\sqrt{2}}(p^0 \pm p^3) \quad \text{and} \quad \mathbf{p}_T = (p^1, p^2). \quad (4)$$

Using these coordinates the  $B$  meson and the two final-state meson momenta can be written as

$$\begin{aligned} P_1 &= \frac{M_B}{\sqrt{2}}(1, 1, \mathbf{0}_T), & P_2 &= \frac{M_B}{\sqrt{2}}(1, r_{\omega(\phi)}^2, \mathbf{0}_T), \\ P_3 &= \frac{M_B}{\sqrt{2}}(0, 1 - r_{\omega(\phi)}^2, \mathbf{0}_T), \end{aligned} \quad (5)$$

respectively, where  $r_{\omega(\phi)}^2 = m_{\omega(\phi)}^2/m_B^2$ ; and the terms proportional to the ratio  $m_{\eta(\phi)}^2/m_B^2$  have been neglected.

For the  $B \rightarrow \omega \eta$  decay considered here, only the  $\omega$  meson's longitudinal part contributes to the decay, its polar vector is  $\epsilon_L = \frac{M_B}{\sqrt{2}M_\omega}(1, -r_\omega^2, \mathbf{0}_T)$ . Putting the light (anti)-quark momenta in the  $B$ ,  $\omega$ , and  $\eta$  meson  $k_1$ ,  $k_2$ , and  $k_3$ , respectively, we can choose

$$\begin{aligned} k_1 &= (x_1 P_1^+, 0, \mathbf{k}_{1T}), & k_2 &= (x_2 P_2^+, 0, \mathbf{k}_{2T}), \\ k_3 &= (0, x_3 P_3^-, \mathbf{k}_{3T}). \end{aligned} \quad (6)$$

Then, the integration over  $k_1^-$ ,  $k_2^-$ , and  $k_3^+$  in Eq. (3) will lead to

$$\mathcal{A}(B \rightarrow \omega \eta) \sim \int dx_1 dx_2 dx_3 b_1 db_1 b_2 db_2 b_3 db_3 \cdot \text{Tr}[C(t)\Phi_B(x_1, b_1)\Phi_\omega(x_2, b_2)\Phi_\eta(x_3, b_3)H(x_i, b_i, t)S_i(x_i)e^{-S(t)}], \quad (7)$$

where  $b_i$  is the conjugate space coordinate of  $k_{iT}$ , and  $t$  is the largest energy scale in the function  $H(x_i, b_i, t)$ . The large logarithms  $\ln(m_W/t)$  are included in the Wilson coefficients  $C(t)$ . The large double logarithms ( $\ln^2 x_i$ ) on the longitudinal direction are summed by the threshold resummation, and they lead to the function  $S_i(x_i)$  which smears the end point singularities on  $x_i$ . The last term,  $e^{-S(t)}$ , is the Sudakov form factor which suppresses the soft dynamics effectively [17]. Thus it makes the perturbative calculation of the hard part  $H$  applicable at an intermediate scale, i.e., the  $M_B$  scale. We will calculate analytically the function  $H(x_i, b_i, t)$  for the considered decays in the first order in an  $\alpha_s$  expansion and give the convoluted amplitudes in the next section.

## A. Wilson coefficients

For the  $B^0 \rightarrow \omega \eta^{(\prime)}$ ,  $B^0 \rightarrow \phi \eta^{(\prime)}$  decays, the related weak effective Hamiltonian  $H_{\text{eff}}$  can be written as [18]

$$\begin{aligned} \mathcal{H}_{\text{eff}} &= \frac{G_F}{\sqrt{2}} \left[ V_{ub} V_{ud}^* (C_1(\mu) O_1^u(\mu) + C_2(\mu) O_2^u(\mu)) \right. \\ &\quad \left. - V_{tb} V_{td}^* \sum_{i=3}^{10} C_i(\mu) O_i(\mu) \right], \end{aligned} \quad (8)$$

where  $C_i(\mu)$  are Wilson coefficients at the renormalization scale  $\mu$  and  $O_i$  are the four-fermion operators. For the  $b \rightarrow d$  transition, for example, these operators can be written as

$$\begin{aligned}
 O_1^{\mu} &= \bar{d}_{\alpha} \gamma^{\mu} L u_{\beta} \cdot \bar{u}_{\beta} \gamma_{\mu} L b_{\alpha}, \\
 O_2^{\mu} &= \bar{d}_{\alpha} \gamma^{\mu} L u_{\alpha} \cdot \bar{u}_{\beta} \gamma_{\mu} L b_{\beta}, \\
 O_3 &= \bar{d}_{\alpha} \gamma^{\mu} L b_{\alpha} \cdot \sum_{q'} \bar{q}'_{\beta} \gamma_{\mu} L q'_{\beta}, \\
 O_4 &= \bar{d}_{\alpha} \gamma^{\mu} L b_{\beta} \cdot \sum_{q'} \bar{q}'_{\beta} \gamma_{\mu} L q'_{\alpha}, \\
 O_5 &= \bar{d}_{\alpha} \gamma^{\mu} L b_{\alpha} \cdot \sum_{q'} \bar{q}'_{\beta} \gamma_{\mu} R q'_{\beta}, \\
 O_6 &= \bar{d}_{\alpha} \gamma^{\mu} L b_{\beta} \cdot \sum_{q'} \bar{q}'_{\beta} \gamma_{\mu} R q'_{\alpha}, \\
 O_7 &= \frac{3}{2} \bar{d}_{\alpha} \gamma^{\mu} L b_{\alpha} \cdot \sum_{q'} e_{q'} \bar{q}'_{\beta} \gamma_{\mu} R q'_{\beta}, \\
 O_8 &= \frac{3}{2} \bar{d}_{\alpha} \gamma^{\mu} L b_{\beta} \cdot \sum_{q'} e_{q'} \bar{q}'_{\beta} \gamma_{\mu} R q'_{\alpha}, \\
 O_9 &= \frac{3}{2} \bar{d}_{\alpha} \gamma^{\mu} L b_{\alpha} \cdot \sum_{q'} e_{q'} \bar{q}'_{\beta} \gamma_{\mu} L q'_{\beta}, \\
 O_{10} &= \frac{3}{2} \bar{d}_{\alpha} \gamma^{\mu} L b_{\beta} \cdot \sum_{q'} e_{q'} \bar{q}'_{\beta} \gamma_{\mu} L q'_{\alpha},
 \end{aligned} \tag{9}$$

where  $\alpha$  and  $\beta$  are the  $SU(3)$  color indices;  $L$  and  $R$  are the left- and right-handed projection operators with  $L = (1 - \gamma_5)$ ,  $R = (1 + \gamma_5)$ . The sum over  $q'$  runs over the quark fields that are active at the scale  $\mu = O(m_b)$ , i.e.,  $q' \in \{u, d, s, c, b\}$ . For the Wilson coefficients  $C_i(\mu)$  ( $i = 1, \dots, 10$ ), we will use the leading order (LO) expressions, although the next-to-leading order (NLO) results already exist in the literature [18]. This is the consistent way to cancel the explicit  $\mu$  dependence in the theoretical formulae. For the renormalization group evolution of the Wilson coefficients from higher scale to lower scale, we use the formulae as given in Ref. [19] directly. At the high  $m_W$  scale, the leading order Wilson coefficients  $C_i(M_W)$  are simple and can be found easily in Ref. [18]. In the pQCD approach, the scale  $t$  may be larger or smaller than the  $m_b$  scale. For the case of  $m_b < t < m_W$ , we evaluate the Wilson coefficients at  $t$  scale using the leading logarithm running equations, as given in Eq. (C1) of Ref. [19]. For the case of  $t < m_b$ , we then evaluate the Wilson coefficients at  $t$  scale by using  $C_i(m_b)$  as input and the formulae given in Appendix D of Ref. [19].

### B. $\phi$ - $\omega$ mixing and $\eta$ - $\eta'$ mixing

For the physical isoscalars  $\phi$  and  $\omega$  meson, we use the ‘‘ideal’’ mixing scheme [20]:

$$\phi(1020) = -s\bar{s}, \quad \omega = \frac{1}{\sqrt{2}}[u\bar{u} + d\bar{d}]. \tag{10}$$

Such an ideal mixing is supported by the known experimental measurements [20].

For the  $\eta$ - $\eta'$  system, there exist two popular mixing basis: the octet-singlet basis and the quark-flavor basis

[21,22]. Here we use the quark-flavor basis [21] and define

$$\eta_q = (u\bar{u} + d\bar{d})/\sqrt{2}, \quad \eta_s = s\bar{s}. \tag{11}$$

The physical states  $\eta$  and  $\eta'$  are related to  $\eta_q$  and  $\eta_s$  through a single mixing angle  $\phi$ ,

$$\begin{pmatrix} \eta \\ \eta' \end{pmatrix} = U(\phi) \begin{pmatrix} \eta_q \\ \eta_s \end{pmatrix} = \begin{pmatrix} \cos\phi & -\sin\phi \\ \sin\phi & \cos\phi \end{pmatrix} \begin{pmatrix} \eta_q \\ \eta_s \end{pmatrix}. \tag{12}$$

The corresponding decay constants  $f_q$ ,  $f_s$ ,  $f_{\eta}^{q,s}$ , and  $f_{\eta'}^{q,s}$  have been defined in Ref. [21] as

$$\langle 0 | \bar{q} \gamma^{\mu} \gamma_5 q | \eta_q(P) \rangle = -\frac{i}{\sqrt{2}} f_q P^{\mu}, \tag{13}$$

$$\langle 0 | \bar{s} \gamma^{\mu} \gamma_5 s | \eta_s(P) \rangle = -i f_s P^{\mu},$$

$$\langle 0 | \bar{q} \gamma^{\mu} \gamma_5 q | \eta^{(\prime)}(P) \rangle = -\frac{i}{\sqrt{2}} f_{\eta^{(\prime)}}^q P^{\mu}, \tag{14}$$

$$\langle 0 | \bar{s} \gamma^{\mu} \gamma_5 s | \eta^{(\prime)}(P) \rangle = -i f_{\eta^{(\prime)}}^s P^{\mu},$$

while the decay constants  $f_{\eta}^{q,s}$  and  $f_{\eta'}^{q,s}$  are related to  $f_q$  and  $f_s$  via the same mixing matrix,

$$\begin{pmatrix} f_{\eta}^q & f_{\eta}^s \\ f_{\eta'}^q & f_{\eta'}^s \end{pmatrix} = U(\phi) \begin{pmatrix} f_q & 0 \\ 0 & f_s \end{pmatrix}. \tag{15}$$

The three input parameters  $f_q$ ,  $f_s$ , and  $\phi$  in the quark-flavor basis have been extracted from various related experiments [21,22]

$$\begin{aligned}
 f_q &= (1.07 \pm 0.02) f_{\pi}, & f_s &= (1.34 \pm 0.06) f_{\pi}, \\
 \phi &= 39.3^{\circ} \pm 1.0^{\circ},
 \end{aligned} \tag{16}$$

where  $f_{\pi} = 130$  MeV. In the numerical calculations, we will use these mixing parameters as inputs.

Although  $\eta$  and  $\eta'$  are generally considered as a linear combination of light quark pairs  $u\bar{u}$ ,  $d\bar{d}$ , and  $s\bar{s}$ , it should be noted that the gluonic content of the  $\eta'$  meson may be needed to interpret the anomalously large branching ratios of  $B \rightarrow K \eta'$  and  $J/\Psi \rightarrow \eta' \gamma$  [4,23]. For  $B \rightarrow (\rho, \pi) \eta^{(\prime)}$  decays, however, the good agreement between the pQCD predictions [5,6] and the measured values for their branching ratios suggest that the gluonic contribution of the  $\eta^{(\prime)}$  meson should be small. In Ref. [9], very recently, the authors calculated the flavor-singlet contribution to the  $B \rightarrow \eta^{(\prime)}$  transition form factors from the gluonic content of the  $\eta^{(\prime)}$  meson. They found that the gluonic contribution is small for both  $B \rightarrow \eta$  and  $B \rightarrow \eta'$  form factors.

Of course, more studies are needed to provide a reliable and precision calculation for the gluonic contribution to the final state involving the  $\eta^{(\prime)}$  meson. For the sake of sim-

plicity, we here first neglect the possible gluonic content of the  $\eta$  and  $\eta'$  meson, and use the quark-flavor mixing scheme for the  $\eta$  and  $\eta'$  meson as defined in Eq. (12). We will calculate the effects of a nonzero gluonic admixture of  $\eta'$  in the next section, and treat them as one kind of theoretical uncertainties.

### C. Wave functions

Now we present the wave functions to be used in the integration. For the wave function of the heavy  $B$  meson, we take

$$\Phi_B = \frac{1}{\sqrt{2N_c}} [(\not{p}_B + M_B)\gamma_5 \phi_B(\mathbf{k}_1)]. \quad (17)$$

Here only the contribution of the Lorentz structure  $\phi_B(\mathbf{k}_1)$  is taken into account, since the contribution of the second Lorentz structure  $\bar{\phi}_B$  is numerically small [24,25] and has been neglected. For the distribution amplitude  $\phi_B$  in Eq. (17), we adopt the model

$$\phi_B(x, b) = N_B x^2 (1-x)^2 \exp\left[-\frac{M_B^2 x^2}{2\omega_b^2} - \frac{1}{2}(\omega_b b)^2\right], \quad (18)$$

where  $\omega_b$  is a free parameter and we take  $\omega_b = 0.4 \pm 0.04$  GeV in numerical calculations, and  $N_B = 91.745$  is the normalization factor for  $\omega_b = 0.4$ . This is the same wave function as is being used in Refs. [19,24], which is a best fit for most of the measured hadronic  $B$  decays.

The wave function for  $d\bar{d}$  components of the  $\eta^{(l)}$  meson is given by [4]

$$\Phi_{\eta_{d\bar{d}}}(p, x, \zeta) \equiv \frac{i\gamma_5}{\sqrt{2N_c}} [\not{p}\phi_{\eta_{d\bar{d}}}^A(x) + m_0^{\eta_{d\bar{d}}}\phi_{\eta_{d\bar{d}}}^P(x) + \zeta m_0^{\eta_{d\bar{d}}}(\not{p}\not{x} - \mathbf{v} \cdot \mathbf{n})\phi_{\eta_{d\bar{d}}}^T(x)], \quad (19)$$

where  $p$  and  $x$  are the momentum and the momentum fraction of  $\eta_{d\bar{d}}$ , respectively, while  $\phi_{\eta_{d\bar{d}}}^A$ ,  $\phi_{\eta_{d\bar{d}}}^P$ , and  $\phi_{\eta_{d\bar{d}}}^T$  represent the axial vector, pseudoscalar, and tensor components of the wave function, respectively. Following Ref. [4], we here also assume that the wave function of  $\eta_{d\bar{d}}$  is the same as the  $\pi$  wave function based on SU(3) flavor symmetry. The parameter  $\zeta$  is either +1 or -1 depending on the assignment of the momentum fraction  $x$ . We also assume that the wave function of the  $u\bar{u}$  component is the same as the wave function of  $d\bar{d}$  based on the isospin symmetry between the up and down quark. For the wave function of the  $s\bar{s}$  component, we also use the same form as given in Eq. (19) for the  $d\bar{d}$  component but with different chiral enhancement and some other changes to be specified later.

The explicit expressions of chiral enhancement scales  $m_0^q = m_0^{\eta_{d\bar{d}}} = m_0^{\eta_{u\bar{u}}}$  and  $m_0^s = m_0^{\eta_{s\bar{s}}}$  are given by [9]

$$m_0^q \equiv \frac{m_{qq}^2}{2m_q} = \frac{1}{2m_q} \left[ m_{\eta'}^2 \cos^2 \phi + m_{\eta}^2 \sin^2 \phi - \frac{\sqrt{2}f_s}{f_q} (m_{\eta'}^2 - m_{\eta}^2) \cos \phi \sin \phi \right], \quad (20)$$

$$m_0^s \equiv \frac{m_{ss}^2}{2m_s} = \frac{1}{2m_s} \left[ m_{\eta'}^2 \cos^2 \phi + m_{\eta}^2 \sin^2 \phi - \frac{f_q}{\sqrt{2}f_s} (m_{\eta'}^2 - m_{\eta}^2) \cos \phi \sin \phi \right], \quad (21)$$

and numerically

$$m_0^q = 1.07 \text{ MeV}, \quad m_0^s = 1.92 \text{ GeV} \quad (22)$$

for  $m_{\eta} = 547.5$  MeV,  $m_{\eta'} = 957.8$  MeV,  $f_q = 1.07f_{\pi}$ ,  $f_s = 1.34f_{\pi}$ , and  $\phi = 39.3^\circ$ .

For the distribution amplitude  $\phi_{\eta_q}^A$ ,  $\phi_{\eta_q}^P$ , and  $\phi_{\eta_q}^T$ , we utilize the results for the  $\pi$  meson obtained from the light cone sum rule [26] including twist-3 contributions:

$$\begin{aligned} \phi_{\eta_{q(s)}}^A(x) &= \frac{3}{\sqrt{2N_c}} f_{q(s)} x(1-x) \\ &\times \left\{ 1 + a_2^{\eta_{q(s)}} \frac{3}{2} [5(1-2x)^2 - 1] \right. \\ &\left. + a_4^{\eta_{q(s)}} \frac{15}{8} [21(1-2x)^4 - 14(1-2x)^2 + 1] \right\}, \end{aligned} \quad (23)$$

$$\begin{aligned} \phi_{\eta_{q(s)}}^P(x) &= \frac{1}{2\sqrt{2N_c}} f_{q(s)} \left\{ 1 + \frac{1}{2} \left( 30\eta_3 - \frac{5}{2}\rho_{\eta_{q(s)}}^2 \right) \right. \\ &\times [3(1-2x)^2 - 1] + \frac{1}{8} \left( -3\eta_3\omega_3 - \frac{27}{20}\rho_{\eta_{q(s)}}^2 \right. \\ &\left. - \frac{81}{10}\rho_{\eta_{q(s)}}^2 a_2^{\eta_{q(s)}} \right) \\ &\left. \times [35(1-2x)^4 - 30(1-2x)^2 + 3] \right\}, \end{aligned} \quad (24)$$

$$\begin{aligned} \phi_{\eta_{q(s)}}^T(x) &= \frac{3}{\sqrt{2N_c}} f_{q(s)} (1-2x) \left[ \frac{1}{6} + \left( 5\eta_3 - \frac{1}{2}\eta_3\omega_3 \right. \right. \\ &\left. \left. - \frac{7}{20}\rho_{\eta_{q(s)}}^2 - \frac{3}{5}\rho_{\eta_{q(s)}}^2 a_2^{\eta_{q,s}} \right) (10x^2 - 10x + 1) \right], \end{aligned} \quad (25)$$

with the updated Gegenbauer moments [27,28]

$$\begin{aligned} a_2^{\eta_{q(s)}} &= 0.115, & a_4^{\eta_{q(s)}} &= -0.015, \\ \rho_{\eta_q} &= 2m_q/m_{qq}; & \rho_{\eta_s} &= 2m_s/m_{ss}, \\ \eta_3 &= 0.015, & \omega_3 &= -3.0. \end{aligned} \quad (26)$$

For  $B \rightarrow \omega \eta^{(l)}$  and  $\phi \eta^{(l)}$  decays, only the longitudinal polarized component  $\Phi_V^L$  for  $V = (\omega, \phi)$  will contribute. The wave function  $\Phi_\omega^L$ , for example, can be written as

$$\Phi_\omega^L = \frac{1}{\sqrt{2N_c}} [m_\omega \not{\epsilon}_L \phi_\omega(x) + \not{\epsilon}_L \not{p} \phi'_\omega(x) + m_\omega I \phi_\omega^s(x)], \quad (27)$$

where the  $\epsilon_L$  and  $\mathbf{p}$  is the polarization vector and the momentum of the  $\omega$  meson, the first term in the above equation is the leading twist wave function (twist-2), while the second and third terms are subleading twist (twist-3) wave functions. For the case of  $V = \phi$ , its wave function is the same in structure as that defined in Eq. (27), but with different mass and distribution amplitudes.

For the light meson wave function, we neglect the  $b$  dependent part, which is not important in numerical analysis. The distribution amplitudes  $\phi_\phi(x)$  and  $\phi_\phi^{t,s}(x)$  are given by [29]

$$\phi_\phi(x) = \frac{3}{\sqrt{6}} f_\phi x(1-x), \quad (28)$$

$$\phi_\phi^t(x) = \frac{f_\phi^T}{2\sqrt{6}} \left\{ 3(1-2x)^2 + 1.68C_4^{1/2}(1-2x) + 0.69 \left[ 1 + (1-2x) \ln \frac{x}{1-x} \right] \right\}, \quad (29)$$

$$\phi_\phi^s(x) = \frac{3}{4\sqrt{6}} f_\phi^T \left[ 3(1-2x)(4.5 - 11.2x + 11.2x^2) + 1.38 \ln \frac{x}{1-x} \right]. \quad (30)$$

For the  $\omega$  meson wave function, we use [30,31]

$$\phi_\omega(x) = \frac{3}{\sqrt{6}} f_\omega x(1-x) [1 + 0.18C_2^{3/2}(1-2x)], \quad (31)$$

$$\phi'_\omega(x) = \frac{f_\omega^T}{2\sqrt{6}} \{ 3(1-2x)^2 + 0.3(1-2x)^2 [5(1-2x)^2 - 3] + 0.21[3 - 30(1-2x)^2 + 35(1-2x)^4] \}, \quad (32)$$

$$\phi_\omega^s(x) = \frac{3}{2\sqrt{6}} f_\omega^T (1-2x) [1 + 0.76(10x^2 - 10x + 1)]. \quad (33)$$

The relevant Gegenbauer polynomials are defined by [29]

$$C_2^{3/2}(t) = \frac{3}{2}(5t^2 - 1), \quad (34)$$

$$C_4^{1/2}(t) = \frac{1}{8}(35t^4 - 30t^2 + 3). \quad (35)$$

### III. PERTURBATIVE CALCULATIONS

In this section, we will calculate and show the decay amplitude for each diagram including wave functions. The hard part  $H(t)$  involves the four quark operators and the necessary hard gluon connecting the four quark operator and the spectator quark. We first consider the  $B \rightarrow \omega \eta$  decay, and then extend the calculation to other decay modes. Analogous to the  $B \rightarrow \rho \eta^{(\prime)}$  decays in [5], there are also eight type diagrams contributing to the  $B \rightarrow \omega \eta$  and  $\omega \eta'$  decay, as illustrated in Fig. 1.

For the  $B \rightarrow \omega \eta$  decay, we first consider the usual factorizable diagrams 1(a) and 1(b). The operators  $O_{1,2}$  and  $O_{3,4,9,10}$  are  $(V-A)(V-A)$  currents; the sum of their amplitudes is given by

$$F_e = 4\sqrt{2}\pi G_F C_F m_B^4 \int_0^1 dx_1 dx_3 \int_0^\infty b_1 db_1 b_3 db_3 \phi_B(x_1, b_1) \{ [(1+x_3)\phi_\eta^A(x_3, b_3) + (1-2x_3)r_\eta(\phi_\eta^P(x_3, b_3) + \phi_\eta^T(x_3, b_3))] \alpha_s(t_e^1) h_e(x_1, x_3, b_1, b_3) \exp[-S_{ab}(t_e^1)] + 2r_\eta \phi_\eta^P(x_3, b_3) \alpha_s(t_e^2) h_e(x_3, x_1, b_3, b_1) \exp[-S_{ab}(t_e^2)] \}, \quad (36)$$

where the ratio  $r_\eta = m_\eta^0/m_B$  with  $m_\eta^0 = m_\eta^q$  or  $m_\eta^s$  as defined in Eqs. (20) and (21); the color factor  $C_F = 4/3$ ,  $\phi_B$  and  $\phi_\eta^{A,P,T}$  are the light cone distribution amplitudes (LCDAs) of the heavy  $B$  meson and the light  $\eta$  meson. The functions  $h_e$ , the scales  $t_e^i$ , and the Sudakov factors  $S_{ab}$  will be given explicitly in the appendix.

The operators  $O_{5,6,7,8}$  have the structure of  $(V-A) \times (V+A)$ . In some decay channels, some of these operators contribute to the decay amplitude in a factorizable way. Since only the vector part of the  $(V+A)$  current contributes to the vector meson production,  $\langle \eta | V-A | B \rangle \langle \omega | V+A | 0 \rangle = \langle \eta | V-A | B \rangle \langle \omega | V-A | 0 \rangle$ , that is

$$F_e^{P1} = F_e. \quad (37)$$

For other cases, one needs to do a Fierz transformation for the corresponding operators to get the right flavor and color structure for factorization to work. We may get  $(S+P) \times (S-P)$  operators from  $(V-A)(V+A)$  ones. Because neither scalar nor the pseudoscalar density give contribution to a vector meson production,  $\langle \omega | S+P | 0 \rangle = 0$ , we get  $F_e^{P2} = 0$ .

For the nonfactorizable diagrams 1(c) and 1(d), all three meson wave functions are involved. The integration of  $b_3$  can be performed using the  $\delta$  function  $\delta(b_3 - b_1)$ , leaving only integration of  $b_1$  and  $b_2$ . The decay amplitude for  $(V-A)(V-A)$  and  $(V-A)(V+A)$  operators can be written as

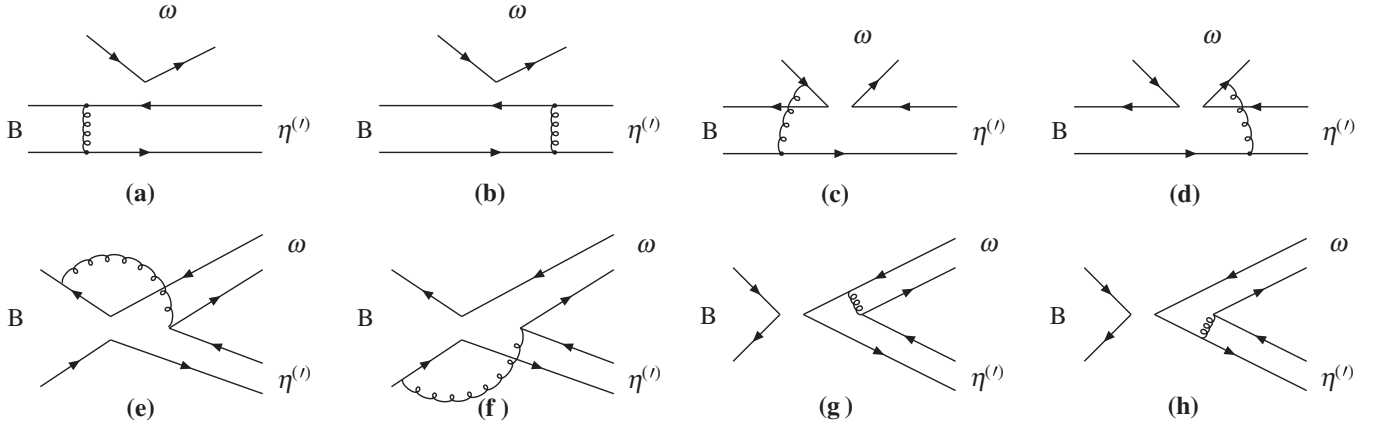


FIG. 1. Feynman diagrams contributing to the  $B \rightarrow \omega \eta^{(\prime)}$  decays when the  $\eta^{(\prime)}$  meson picks up the spectator quark, where diagram (a) and (b) contribute to the  $B \rightarrow \eta^{(\prime)}$  form factor  $F_{0,1}^{B \rightarrow \eta^{(\prime)}}$ .

$$M_e = -M_e^{P2} = \frac{16}{\sqrt{3}} G_F \pi C_F m_B^4 \int_0^1 dx_1 dx_2 dx_3 \int_0^\infty b_1 db_1 b_2 db_2 \phi_B(x_1, b_1) \phi_\omega(x_2, b_2) \times \{ [2x_3 r_\eta \phi_\eta^T(x_3, b_1) - x_3 \phi_\eta^A(x_3, b_1)] \alpha_s(t_f) h_f(x_1, x_2, x_3, b_1, b_2) \exp[-S_{cd}(t_f)] \}, \quad (38)$$

$$M_e^{P1} = -\frac{32}{\sqrt{3}} G_F \pi C_F r_\omega m_B^4 \int_0^1 dx_1 dx_2 dx_3 \int_0^\infty b_1 db_1 b_2 db_2 \phi_B(x_1, b_1) \{ [x_2 \phi_\eta^A(x_3, b_1) (\phi_\omega^s(x_2, b_2) - \phi_\omega^t(x_2, b_2)) + r_\eta ((x_2 + x_3) (\phi_\eta^p(x_3, b_1) \phi_\omega^s(x_2, b_2) + \phi_\eta^T(x_3, b_1) \phi_\omega^t(x_2, b_2)) + (x_3 - x_2) (\phi_\eta^p(x_3, b_1) \phi_\omega^t(x_2, b_2) + \phi_\eta^T(x_3, b_1) \phi_\omega^s(x_2, b_2)))] \alpha_s(t_f) h_f(x_1, x_2, x_3, b_1, b_2) \exp[-S_{cd}(t_f)] \}. \quad (39)$$

For the nonfactorizable annihilation diagrams 1(e) and 1(f), there are three kinds of decay amplitudes. For the  $(V - A)(V - A)$  operators, the decay amplitude  $M_a$  is

$$M_a = \frac{16}{\sqrt{3}} \pi G_F C_F m_B^4 \int_0^1 dx_1 dx_2 dx_3 \int_0^\infty b_1 db_1 b_2 db_2 \phi_B(x_1, b_1) \times \{ [r_\omega r_\eta (x_3 - x_2) [\phi_\eta^p(x_3, b_2) \phi_\omega^t(x_2, b_2) + \phi_\eta^T(x_3, b_2) \phi_\omega^s(x_2, b_2)] + r_\omega r_\eta (x_2 + x_3) \times [\phi_\eta^p(x_3, b_2) \phi_\omega^s(x_2, b_2) + \phi_\eta^T(x_3, b_2) \phi_\omega^t(x_2, b_2)] + x_3 \phi_\omega(x_2, b_2) \phi_\eta^A(x_3, b_2)] \alpha_s(t_f^4) h_f^4(x_1, x_2, x_3, b_1, b_2) \times \exp[-S_{ef}(t_f^4)] - [r_\omega r_\eta (x_2 - x_3) [\phi_\eta^p(x_3, b_2) \phi_\omega^t(x_2, b_2) + \phi_\eta^T(x_3, b_2) \phi_\omega^s(x_2, b_2)] + r_\omega r_\eta [(2 + x_2 + x_3) \phi_\eta^p(x_3, b_2) \phi_\omega^s(x_2, b_2) - (2 - x_2 - x_3) \phi_\eta^T(x_3, b_2) \phi_\omega^t(x_2, b_2)] + x_2 \phi_\omega(x_2, b_2) \phi_\eta^A(x_3, b_2)] \times \alpha_s(t_f^3) h_f^3(x_1, x_2, x_3, b_1, b_2) \exp[-S_{ef}(t_f^3)] \}. \quad (40)$$

For the  $(V - A)(V + A)$  and  $(S - P)(S + P)$  operators, we have

$$M_a^{P1} = \frac{16}{\sqrt{3}} G_F \pi C_F m_B^4 \int_0^1 dx_1 dx_2 dx_3 \int_0^\infty b_1 db_1 b_2 db_2 \phi_B(x_1, b_1) \{ [x_2 r_\omega \phi_\eta^A(x_3, b_2) (\phi_\omega^s(x_2, b_2) + \phi_\omega^t(x_2, b_2)) - x_3 r_\eta (\phi_\eta^p(x_3, b_2) + \phi_\eta^T(x_3, b_2)) \phi_\omega(x_2, b_2)] \alpha_s(t_f^4) h_f^4(x_1, x_2, x_3, b_1, b_2) \exp[-S_{ef}(t_f^4)] + [(2 - x_2) r_\omega \phi_\eta^A(x_3, b_2) (\phi_\omega^s(x_2, b_2) + \phi_\omega^t(x_2, b_2)) - (2 - x_3) r_\eta (\phi_\eta^p(x_3, b_2) + \phi_\eta^T(x_3, b_2)) \phi_\omega(x_2, b_2)] \times \alpha_s(t_f^3) h_f^3(x_1, x_2, x_3, b_1, b_2) \exp[-S_{ef}(t_f^3)] \}, \quad (41)$$

$$\begin{aligned}
 M_a^{P2} = & -\frac{16}{\sqrt{3}} \pi G_F C_F m_B^4 \int_0^1 dx_1 dx_2 dx_3 \int_0^\infty b_1 db_1 b_2 db_2 \phi_B(x_1, b_1) \{ [x_2 \phi_\omega(x_2, b_2) \phi_\eta^A(x_3, b_2) \\
 & + r_\omega r_\eta ((x_2 - x_3) (\phi_\eta^P(x_3, b_2) \phi_\omega^t(x_2, b_2) + \phi_\eta^T(x_3, b_2) \phi_\omega^s(x_2, b_2)) + (x_2 + x_3) (\phi_\eta^P(x_3, b_2) \phi_\omega^s(x_2, b_2) \\
 & + \phi_\eta^T(x_3, b_2) \phi_\omega^t(x_2, b_2))] \alpha_s(t_f^4) h_f^4(x_1, x_2, x_3, b_1, b_2) \exp[-S_{ef}(t_f^4)] - [x_3 \phi_\omega(x_2, b_2) \phi_\eta^A(x_3, b_2) \\
 & + r_\omega r_\eta ((x_3 - x_2) (\phi_\eta^P(x_3, b_2) \phi_\omega^t(x_2, b_2) + \phi_\eta^T(x_3, b_2) \phi_\omega^s(x_2, b_2)) + (2 + x_2 + x_3) \phi_\eta^P(x_3, b_2) \phi_\omega^s(x_2, b_2) \\
 & - (2 - x_2 - x_3) \phi_\eta^T(x_3, b_2) \phi_\omega^t(x_2, b_2))] \alpha_s(t_f^3) h_f^3(x_1, x_2, x_3, b_1, b_2) \exp[-S_{ef}(t_f^3)] \}. \quad (42)
 \end{aligned}$$

The factorizable annihilation diagrams 1(g) and 1(h) involve only  $\eta$  and  $\omega$  wave functions. There are also three kinds of decay amplitudes:  $F_a$  is for  $(V - A)(V - A)$  type operators,  $F_a^{P1}$  and  $F_a^{P2}$  are for  $(V - A)(V + A)$  and  $(S - P)(S + P)$  type operators, respectively:

$$\begin{aligned}
 F_a = -F_a^{P1} = & -4\sqrt{2} G_F \pi C_F m_B^4 \int_0^1 dx_2 dx_3 \int_0^\infty b_2 db_2 b_3 db_3 \{ [x_3 \phi_\eta^A(x_3, b_3) \phi_\omega(x_2, b_2) \\
 & + 2r_\omega r_\eta ((x_3 + 1) \phi_\eta^P(x_3, b_3) + (x_3 - 1) \phi_\eta^t(x_3, b_3)) \phi_\omega^s(x_2, b_2)] \alpha_s(t_e^3) h_a(x_2, x_3, b_2, b_3) \exp[-S_{gh}(t_e^3)] \\
 & - [x_2 \phi_\eta^A(x_3, b_3) \phi_\omega(x_2, b_2) + 2r_\eta r_\omega ((x_2 + 1) \phi_\omega^s(x_2, b_2) + (x_2 - 1) \phi_\omega^t(x_2, b_2)) \phi_\eta^P(x_3, b_3)] \alpha_s(t_e^4) h_a(x_3, x_2, b_3, b_2) \\
 & \times \exp[-S_{gh}(t_e^4)] \}, \quad (43)
 \end{aligned}$$

$$\begin{aligned}
 F_a^{P2} = & -8\sqrt{2} G_F \pi C_F m_B^4 \int_0^1 dx_2 dx_3 \int_0^\infty b_2 db_2 b_3 db_3 \{ [x_3 r_\eta (\phi_\eta^P(x_3, b_3) - \phi_\eta^t(x_3, b_3)) \phi_\omega(x_2, b_2) \\
 & + 2r_\omega \phi_\eta^A(x_3, b_3) \phi_\omega^s(x_2, b_2)] \alpha_s(t_e^3) h_a(x_2, x_3, b_2, b_3) \exp[-S_{gh}(t_e^3)] + [x_2 r_\omega (\phi_\omega^s(x_2, b_2) - \phi_\omega^t(x_2, b_2)) \phi_\eta^A(x_3, b_3) \\
 & + 2r_\eta \phi_\omega(x_2, b_2) \phi_\eta^P(x_3, b_3)] \alpha_s(t_e^4) h_a(x_3, x_2, b_3, b_2) \exp[-S_{gh}(t_e^4)] \}. \quad (44)
 \end{aligned}$$

In the above equations, we have assumed that  $x_1 \ll (x_2, x_3)$ . Since the light quark momentum fraction  $x_1$  in the  $B$  meson is peaked at the small region, while quark momentum fraction  $x_3$  of  $\eta$  is peaked around 0.5, this is not a bad approximation. The numerical results also show that this approximation makes very little difference in the final result.

By exchanging the position of  $\eta^{(\prime)}$  and  $\omega$  in Fig. 1, one finds the new Feynman diagrams are illustrated in Fig. 2. Just like the case of Fig. 1, we first consider the factorizable diagrams 2(a) and 2(b). The decay amplitude  $F_e$  induced by inserting the  $(V - A)(V - A)$  operators is

$$\begin{aligned}
 F_{e\omega} = & 4\sqrt{2} G_F \pi C_F m_B^4 \int_0^1 dx_1 dx_3 \int_0^\infty b_1 db_1 b_3 db_3 \phi_B(x_1, b_1) \{ [(1 + x_3) \phi_\omega(x_3, b_3) + (1 - 2x_3) r_\omega (\phi_\omega^s(x_3, b_3) \\
 & + \phi_\omega^t(x_3, b_3))] \alpha_s(t_e^1) h_e(x_1, x_3, b_1, b_3) \exp[-S_{ab}(t_e^1)] + 2r_\omega \phi_\omega^s(x_3, b_3) \alpha_s(t_e^2) h_e(x_3, x_1, b_3, b_1) \exp[-S_{ab}(t_e^2)] \}. \quad (45)
 \end{aligned}$$

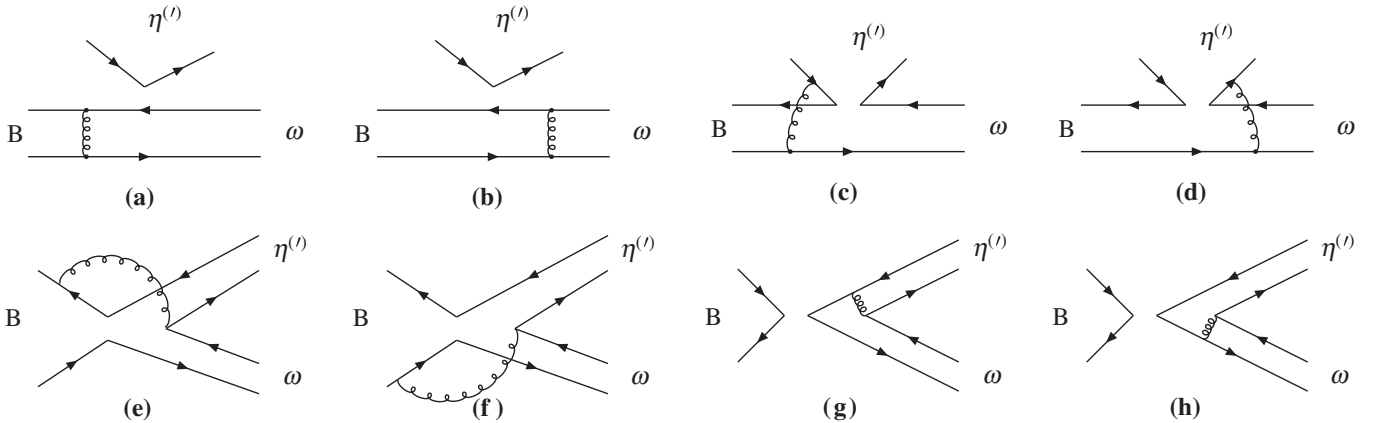


FIG. 2. Feynman diagrams contributing to the  $B \rightarrow \omega \eta^{(\prime)}$  decays when the  $\omega$  boson picks up the spectator quark.

Figures 2(a) and 2(b) are also the diagrams being used to extract the form factor  $A_0^{B \rightarrow \omega}$ . According to the definition in Ref. [25], we can extract  $A_0^{B \rightarrow \omega}$  from Eq. (45).

From Figs. 2(a) and 2(b), it is easy to find the decay amplitude  $F_{e\omega}^{P1}$  and  $F_{e\omega}^{P2}$ :

$$F_{e\omega}^{P1} = -F_{e\omega}, \quad (46)$$

$$\begin{aligned} F_{e\omega}^{P2} = & 8\sqrt{2}G_F\pi C_F r_\eta m_B^4 \int_0^1 dx_1 dx_3 \int_0^\infty b_1 db_1 b_3 db_3 \phi_B(x_1, b_1) \{ [\phi_\omega(x_3, b_3) + r_\omega((x_3 + 2)\phi_\omega^s(x_3, b_3) - x_3\phi_\omega'(x_3, b_3))] \\ & \times \alpha_s(t_e^1) h_e(x_1, x_3, b_1, b_3) \exp[-S_{ab}(t_e^1)] + (x_1\phi_\omega(x_3, b_3) + 2r_\omega\phi_\omega^s(x_3, b_3))\alpha_s(t_e^2) h_e(x_3, x_1, b_3, b_1) \exp[-S_{ab}(t_e^2)] \}. \end{aligned} \quad (47)$$

For the nonfactorizable diagrams 2(c) and 2(d), the corresponding decay amplitudes are

$$\begin{aligned} M_{e\omega} = & -\frac{16}{\sqrt{3}}G_F\pi C_F m_B^4 \int_0^1 dx_1 dx_2 dx_3 \int_0^\infty b_1 db_1 b_2 db_2 \phi_B(x_1, b_1) \phi_\eta^A(x_2, b_2) \\ & \times \{ x_3[\phi_\omega(x_3, b_1) - 2r_\omega\phi_\omega'(x_3, b_1)]\alpha_s(t_f) h_f(x_1, x_2, x_3, b_1, b_2) \exp[-S_{cd}(t_f)] \}, \end{aligned} \quad (48)$$

and

$$M_{e\omega}^{P1} = 0, \quad M_{e\omega}^{P2} = M_{e\omega}. \quad (49)$$

For the nonfactorizable annihilation diagrams 2(e) and 2(f), again all three wave functions are involved. The three kinds of decay amplitudes are of the form

$$\begin{aligned} M_{a\omega} = & \frac{16}{\sqrt{3}}G_F\pi C_F m_B^4 \int_0^1 dx_1 dx_2 dx_3 \int_0^\infty b_1 db_1 b_2 db_2 \phi_B(x_1, b_1) \{ [x_3\phi_\omega(x_3, b_2)\phi_\eta^A(x_2, b_2) \\ & + r_\omega r_\eta((x_3 - x_2)(\phi_\eta^P(x_2, b_2)\phi_\omega'(x_3, b_2) + \phi_\eta^T(x_2, b_2)\phi_\omega^s(x_3, b_2)) + (x_3 + x_2)(\phi_\eta^P(x_2, b_2)\phi_\omega^s(x_3, b_2) \\ & + \phi_\eta^T(x_2, b_2)\phi_\omega'(x_3, b_2))] \alpha_s(t_f^4) h_f^4(x_1, x_2, x_3, b_1, b_2) \exp[-S_{ef}(t_f^4)] - [x_2\phi_\omega(x_3, b_2)\phi_\eta^A(x_2, b_2) \\ & + r_\omega r_\eta((x_2 - x_3)(\phi_\eta^P(x_2, b_2)\phi_\omega'(x_3, b_2) + \phi_\eta^T(x_2, b_2)\phi_\omega^s(x_3, b_2)) + r_\omega r_\eta((2 + x_2 + x_3)\phi_\eta^P(x_2, b_2)\phi_\omega^s(x_3, b_2) \\ & - (2 - x_2 - x_3)\phi_\eta^T(x_2, b_2)\phi_\omega'(x_3, b_2))] \alpha_s(t_f^3) h_f^3(x_1, x_2, x_3, b_1, b_2) \exp[-S_{ef}(t_f^3)] \}, \end{aligned} \quad (50)$$

$$\begin{aligned} M_{a\omega}^{P1} = & -\frac{16}{\sqrt{3}}G_F\pi C_F m_B^4 \int_0^1 dx_1 dx_2 dx_3 \int_0^\infty b_1 db_1 b_2 db_2 \phi_B(x_1, b_1) \{ [x_2 r_\eta \phi_\omega(x_3, b_2)(\phi_\eta^P(x_2, b_2) + \phi_\eta^T(x_2, b_2)) \\ & - x_3 r_\omega(\phi_\omega^s(x_3, b_2) + \phi_\omega'(x_3, b_2))\phi_\eta^A(x_2, b_2)] \alpha_s(t_f^4) h_f^4(x_1, x_2, x_3, b_1, b_2) \exp[-S_{ef}(t_f^4)] \\ & + [(2 - x_2)r_\eta \phi_\omega(x_3, b_2)(\phi_\eta^P(x_2, b_2) + \phi_\eta^T(x_2, b_2)) - (2 - x_3)r_\omega(\phi_\omega^s(x_3, b_2) + \phi_\omega'(x_3, b_2))\phi_\eta^A(x_2, b_2)] \\ & \times \alpha_s(t_f^3) h_f^3(x_1, x_2, x_3, b_1, b_2) \exp[-S_{ef}(t_f^3)] \}, \end{aligned} \quad (51)$$

$$\begin{aligned} M_{a\omega}^{P2} = & -\frac{16}{\sqrt{3}}\pi G_F C_F m_B^4 \int_0^1 dx_1 dx_2 dx_3 \int_0^\infty b_1 db_1 b_2 db_2 \phi_B(x_1, b_1) \{ [x_2\phi_\omega(x_3, b_2)\phi_\eta^A(x_2, b_2) \\ & + r_\omega r_\eta((x_2 - x_3)(\phi_\eta^P(x_2, b_2)\phi_\omega'(x_3, b_2) + \phi_\eta^T(x_2, b_2)\phi_\omega^s(x_3, b_2)) + (x_2 + x_3)(\phi_\eta^P(x_2, b_2)\phi_\omega^s(x_3, b_2) \\ & + \phi_\eta^T(x_2, b_2)\phi_\omega'(x_3, b_2))] \alpha_s(t_f^4) h_f^4(x_1, x_2, x_3, b_1, b_2) \exp[-S_{ef}(t_f^4)] - [x_3\phi_\omega(x_3, b_2)\phi_\eta^A(x_2, b_2) \\ & + r_\omega r_\eta((x_3 - x_2)(\phi_\eta^P(x_2, b_2)\phi_\omega'(x_3, b_2) + \phi_\eta^T(x_2, b_2)\phi_\omega^s(x_3, b_2)) + (2 + x_2 + x_3)\phi_\eta^P(x_2, b_2)\phi_\omega^s(x_3, b_2) \\ & - (2 - x_2 - x_3)\phi_\eta^T(x_2, b_2)\phi_\omega'(x_3, b_2))] \alpha_s(t_f^3) h_f^3(x_1, x_2, x_3, b_1, b_2) \exp[-S_{ef}(t_f^3)] \}. \end{aligned} \quad (52)$$

For the factorizable annihilation diagrams 2(g) and 2(h), we have

$$F_{a\omega} = -F_a, \quad F_{a\omega}^{P1} = -F_a^{P1}, \quad F_{a\omega}^{P2} = -F_a^{P2}. \quad (53)$$

Following the same procedure, it is straightforward to calculate the decay amplitudes for the  $B \rightarrow \phi \eta^{(\prime)}$  decays. It is worth mentioning that all the eight Feynman diagrams in Fig. 1 after the replacements of the  $\omega$  meson by the  $\phi$  meson will contribute to  $B \rightarrow \phi \eta^{(\prime)}$  decays; but Figs. 2(a)–2(d) could not contribute to the same decay since  $\phi = -s\bar{s}$  in the ideal mixing scheme of the  $\omega$ - $\phi$  system.

Combining the contributions from the different diagrams, the total decay amplitude for  $B^0 \rightarrow \omega \eta$  can be written as

$$\begin{aligned} \sqrt{2}\mathcal{M}(\omega\eta) = & F_e F_1(\phi) f_\omega [\xi_u(C_1 + \frac{1}{3}C_2) - \xi_t(\frac{2}{3}C_3 + \frac{5}{3}C_4 + 2C_5 + \frac{2}{3}C_6 + \frac{1}{2}C_7 + \frac{1}{6}C_8 + \frac{1}{3}C_9 - \frac{1}{3}C_{10})] \\ & + M_e F_1(\phi) [\xi_u C_2 - \xi_t(C_3 + 2C_4 - 2C_6 - \frac{1}{2}C_8 - \frac{1}{2}C_9 + \frac{1}{2}C_{10})] \\ & + F_{e\omega} [\xi_u(C_1 + \frac{1}{3}C_2) f_\eta^d - \xi_t(\frac{2}{3}C_3 + \frac{5}{3}C_4 - 2C_5 - \frac{2}{3}C_6 - \frac{1}{2}C_7 - \frac{1}{6}C_8 + \frac{1}{3}C_9 - \frac{1}{3}C_{10}) f_\eta^d \\ & - \xi_t(C_3 + \frac{1}{3}C_4 - C_5 - \frac{1}{3}C_6 + \frac{1}{2}C_7 + \frac{1}{6}C_8 - \frac{1}{2}C_9 - \frac{1}{6}C_{10}) f_\eta^s] + F_{e\bar{\omega}}^2 [-\xi_t(\frac{1}{3}C_5 + C_6 - \frac{1}{6}C_7 - \frac{1}{2}C_8) f_\eta^d] \\ & + M_{e\omega} F_1(\phi) [\xi_u C_2 - \xi_t(C_3 + 2C_4 + 2C_6 + \frac{1}{2}C_8 - \frac{1}{2}C_9 + \frac{1}{2}C_{10})] \\ & + M_{e\omega} F_2(\phi) [-\xi_t(C_4 + C_6 - \frac{1}{2}C_8 - \frac{1}{2}C_{10})] + (M_a + M_{a\omega}) F_1(\phi) [\xi_u C_2 - \xi_t(C_3 + 2C_4 - \frac{1}{2}C_9 + \frac{1}{2}C_{10})] \\ & - (M_e^{P_1} + M_a^{P_1} + M_{a\omega}^{P_1}) F_1(\phi) \xi_t(C_5 - \frac{1}{2}C_7) - (M_a^{P_2} + M_{a\omega}^{P_2}) F_1(\phi) \xi_t(2C_6 + \frac{1}{2}C_8), \end{aligned} \quad (54)$$

where  $\xi_u = V_{ub}^* V_{ud}$ ,  $\xi_t = V_{tb}^* V_{td}$ , and

$$F_1(\phi) = \frac{\cos\phi}{\sqrt{2}}, \quad F_2(\phi) = -\sin\phi, \quad (55)$$

are the mixing factors. The Wilson coefficients  $C_i = C_i(t)$  in Eq. (54) should be calculated at the appropriate scale  $t$  using equations as given in the appendices of Ref. [19].

By doing the replacements of  $f_\omega \rightarrow f_\phi$  and  $\phi_\omega^{A,P,T} \rightarrow \phi_\phi^{A,P,T}$ , one obtains the decay amplitude for the  $B^0 \rightarrow \phi \eta$  decay:

$$\begin{aligned} \mathcal{M}(\phi\eta) = & F_e \xi_t(C_3 + \frac{1}{3}C_4 + C_5 + \frac{1}{3}C_6 - \frac{1}{2}C_7 - \frac{1}{6}C_8 - \frac{1}{2}C_9 - \frac{1}{6}C_{10}) F_1(\phi) + M_e \xi_t(C_4 - C_6 + \frac{1}{2}C_8 - \frac{1}{2}C_{10}) F_1(\phi) \\ & + (M_a + M_{a\phi}) \xi_t(C_4 - \frac{1}{2}C_{10}) F_2(\phi) + (M_a^{P_2} + M_{a\phi}^{P_2}) \xi_t(C_6 - \frac{1}{2}C_8) F_2(\phi). \end{aligned} \quad (56)$$

The complete decay amplitude  $\mathcal{M}(\omega \eta^{(\prime)})$  and  $\mathcal{M}(\phi \eta^{(\prime)})$  can be obtained easily from Eqs. (54) and (56) by the following replacements

$$\begin{aligned} f_\eta^d, f_\eta^s & \rightarrow f_\eta^d, f_\eta^s, \\ F_1(\phi) & \rightarrow F_1^l(\phi) = \frac{\sin\phi}{\sqrt{2}}, \\ F_2(\phi) & \rightarrow F_2^l(\phi) = \cos\phi. \end{aligned} \quad (57)$$

#### IV. NUMERICAL RESULTS AND DISCUSSIONS

In this section, we will present the numerical results of the branching ratios and  $CP$  violating asymmetries for those considered decay modes.

##### A. Input parameters

We show here the input parameters to be used in the numerical calculations.

The masses, decay constants, QCD scale, and  $B^0$  meson lifetime are

$$\begin{aligned} \Lambda_{\overline{\text{MS}}}^{(f=4)} &= 250 \text{ MeV}, & f_\pi &= 130 \text{ MeV}, \\ f_B &= 190 \text{ MeV}, & f_\phi &= 237 \text{ MeV}, \\ f_\phi^T &= 220 \text{ MeV}, & M_W &= 80.41 \text{ GeV}, \\ f_\omega &= 195 \text{ MeV}, & f_\omega^T &= 140 \text{ MeV}, \\ M_\phi &= 1.02 \text{ GeV}, & M_\omega &= 0.78 \text{ GeV}, \\ m_\eta &= 547.5 \text{ MeV}, & m_{\eta'} &= 957.8 \text{ MeV}, \\ M_B &= 5.2792 \text{ GeV}, & \tau_{B^0} &= 1.54 \times 10^{-12} \text{ s}. \end{aligned} \quad (58)$$

For the Cabibbo-Kobayashi-Maskawa (CKM) matrix elements, here we adopt the Wolfenstein parametrization for the CKM matrix up to  $\mathcal{O}(\lambda^5)$  with the parameters  $\lambda = 0.2272$ ,  $A = 0.818$ ,  $\bar{\rho} = 0.221$ , and  $\bar{\eta} = 0.340$  [20].

From Eq. (45) we find the numerical values of the corresponding form factors at zero momentum transfer:  $A_0^{B \rightarrow \omega}(q^2 = 0) = 0.35 \pm 0.05(\omega_b)$  which are consistent with those given in [32].

##### B. Branching ratios

For  $B^0 \rightarrow \omega \eta^{(\prime)}$  and  $\phi \eta^{(\prime)}$  decays, the decay amplitudes as given in Eqs. (54) and (56) can be rewritten as

$$\mathcal{M} = V_{ub}^* V_{ud} T - V_{tb}^* V_{td} P = V_{ub}^* V_{ud} T [1 + z e^{i(\alpha+\delta)}], \quad (59)$$

where

$$z = \left| \frac{V_{tb}^* V_{td}}{V_{ub}^* V_{ud}} \right| \left| \frac{P}{T} \right|, \quad \alpha = \arg \left[ -\frac{V_{td} V_{tb}^*}{V_{ud} V_{ub}^*} \right] \quad (60)$$

are the ratio of penguin to tree contributions and the weak phase (one of the three CKM angles), respectively, and  $\delta$  is the relative strong phase between tree ( $T$ ) and penguin ( $P$ ) diagrams. The  $CP$ -averaged branching ratio for  $B^0 \rightarrow \omega(\phi)\eta^{(\prime)}$  decays can be then written as

$$\begin{aligned} \text{Br} &= (|\mathcal{M}|^2 + |\bar{\mathcal{M}}|^2)/2 \\ &= |V_{ub} V_{ud}^* T|^2 [1 + 2z \cos \alpha \cos \delta + z^2], \end{aligned} \quad (61)$$

where the ratio  $z$  and the strong phase  $\delta$  have been defined in Eqs. (59) and (60).

Using the wave functions and the input parameters as specified in previous sections, it is straightforward to calculate the branching ratios for the four considered decays. We find numerically that

$$\text{Br}(B^0 \rightarrow \omega \eta) = [2.7_{-0.6}^{+0.8}(\omega_b) \pm 0.7(\alpha) \pm 0.3(a_2)] \times 10^{-7}, \quad (62)$$

$$\text{Br}(B^0 \rightarrow \omega \eta') = [0.75_{-0.14}^{+0.19}(\omega_b) + 0.25_{-0.24}(\alpha) + 0.19_{-0.17}(a_2)] \times 10^{-7}. \quad (63)$$

The main errors are induced by the uncertainties of  $\omega_b = 0.4 \pm 0.04$  GeV,  $\alpha = 100^\circ \pm 20^\circ$ , and  $a_2 = 0.115 \pm 0.115$ , respectively.

For the  $B^0 \rightarrow \phi \eta^{(\prime)}$  decays, the decay amplitudes involve only the penguin ( $P$ ) diagrams, the branching ratios are:

$$\text{Br}(B^0 \rightarrow \phi \eta) = [6.3_{-1.0}^{+1.2}(\omega_b) + 2.7_{-1.0}(m_s) + 1.4_{-1.3}(a_2)] \times 10^{-9}, \quad (64)$$

$$\text{Br}(B^0 \rightarrow \phi \eta') = [7.3_{-1.3}^{+1.5}(\omega_b) + 2.3_{-0.9}(m_s) + 2.2_{-2.0}(a_2)] \times 10^{-9}. \quad (65)$$

The main errors are induced by the uncertainties of  $\omega_b = 0.4 \pm 0.04$  GeV,  $m_s = 130 \pm 30$  MeV, and  $a_2 = 0.115 \pm 0.115$ , respectively.

For the  $CP$ -averaged branching ratios of the considered four decays, the pQCD predictions agree within errors with both the experimental upper limits as shown in Eqs. (1) and (2), and the theoretical predictions in the QCDF approach, for example, as given in Ref. [1]:

$$\text{Br}(B^0 \rightarrow \omega \eta) = (0.31_{-0.27}^{+0.46}) \times 10^{-6}, \quad (66)$$

$$\text{Br}(B^0 \rightarrow \omega \eta') = (0.20_{-0.18}^{+0.34}) \times 10^{-6}, \quad (67)$$

$$\text{Br}(B^0 \rightarrow \phi \eta^{(\prime)}) \approx 1 \times 10^{-9}, \quad (68)$$

where the individual errors as given in Refs. [1] have been added in quadrature. It is easy to see that the central values of the pQCD predictions for  $\text{Br}(B \rightarrow \phi \eta^{(\prime)})$  are larger than the corresponding QCDF predictions, although they are still consistent if the large theoretical uncertainties are taken into account. The branching ratios  $\text{Br}(B \rightarrow \omega \eta^{(\prime)})$  at the  $10^{-7}$  level can be measured in the forthcoming LHC experiments [33]. But it is very difficult to measure  $B \rightarrow \phi \eta^{(\prime)}$  decays because of their tiny ( $\sim 10^{-9}$ ) branching ratio, if the pQCD predictions are true.

It is worth stressing that the theoretical predictions in the pQCD approach have large theoretical errors induced by the still large uncertainties of many input parameters. In our analysis, we considered the constraints on these parameters from analysis of other well measured decay channels. From numerical calculations, we get to know that the main errors come from the uncertainty of  $\omega_b$ ,  $m_s$ ,  $\alpha$ , and  $a_2^{\eta^{(\prime)}}$ . Additionally, the final-state interactions remain unsettled in pQCD, which is nonperturbative in nature but not universal.

In Fig. 3 we show the parameter dependence of the pQCD predictions for the branching ratios of  $B \rightarrow \omega \eta$  and  $\omega \eta'$  decays for  $\omega_b = 0.4 \pm 0.04$  GeV,  $\alpha = [0^\circ, 180^\circ]$ . From the numerical results and the figures we observe that the pQCD predictions are sensitive to the variations of  $\omega_b$  and  $\alpha$ .

### C. $CP$ -violating asymmetries

Now we turn to the evaluations of the  $CP$ -violating asymmetries of  $B \rightarrow \omega \eta^{(\prime)}$  decays in pQCD approach. Because these decays are neutral  $B$  meson decays, we should consider the effects of  $B^0$ - $\bar{B}^0$  mixing. For  $B^0$  meson decays into a  $CP$  eigenstate  $f$ , the time-dependent  $CP$ -violating asymmetry can be defined as

$$\begin{aligned} & \frac{\text{Br}(\bar{B}^0(t) \rightarrow f) - \text{Br}(B^0(t) \rightarrow f)}{\text{Br}(\bar{B}^0(t) \rightarrow f) + \text{Br}(B^0(t) \rightarrow f)} \\ & \equiv \mathcal{A}_{CP}^{\text{dir}} \cos(\Delta m t) + \mathcal{A}_{CP}^{\text{mix}} \sin(\Delta m t), \end{aligned} \quad (69)$$

where  $\Delta m$  is the mass difference between the two  $B_d^0$  mass eigenstates,  $t = t_{CP} - t_{\text{tag}}$  is the time difference between the tagged  $B^0$  ( $\bar{B}^0$ ) and the accompanying  $\bar{B}^0$  ( $B^0$ ) with opposite  $b$  flavor decaying to the final  $CP$ -eigenstate  $f_{CP}$  at the time  $t_{CP}$ . The direct and mixing-induced  $CP$ -violating asymmetries  $\mathcal{A}_{CP}^{\text{dir}}$  and  $\mathcal{A}_{CP}^{\text{mix}}$  can be written as

$$\mathcal{A}_{CP}^{\text{dir}} = \frac{|\lambda_{CP}|^2 - 1}{1 + |\lambda_{CP}|^2}, \quad \mathcal{A}_{CP}^{\text{mix}} = \frac{2 \text{Im}(\lambda_{CP})}{1 + |\lambda_{CP}|^2}, \quad (70)$$

where the  $CP$ -violating parameter  $\lambda_{CP}$  is

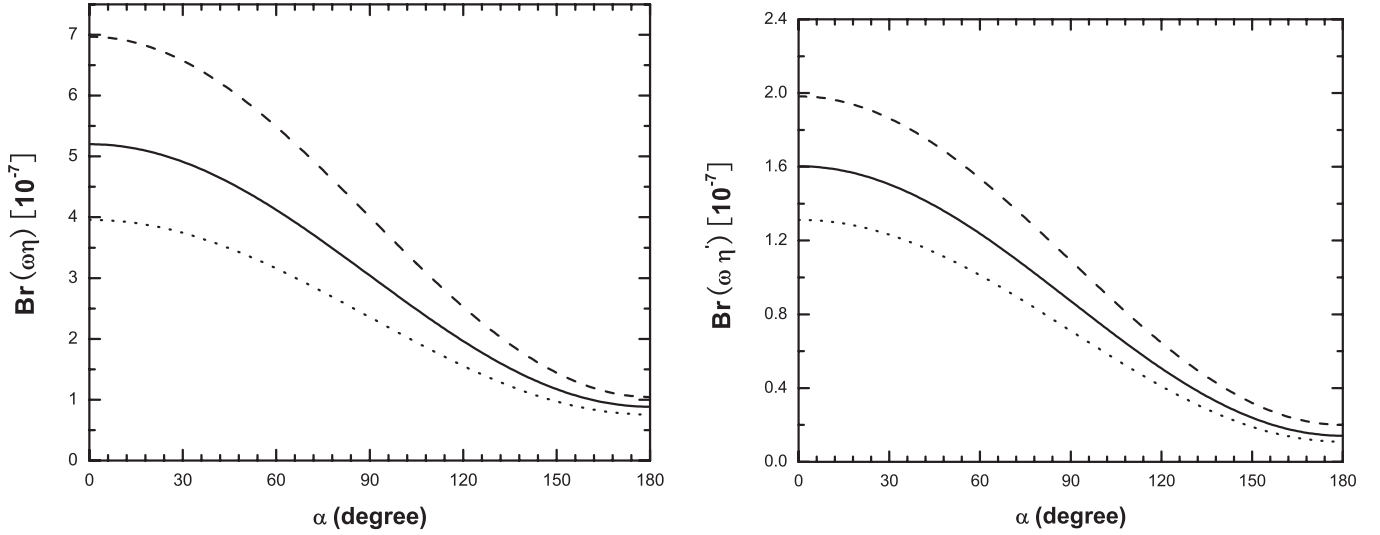


FIG. 3. The  $\alpha$  dependence of the branching ratios (in unit of  $10^{-7}$ ) of  $B^0 \rightarrow \omega \eta$  and  $\omega \eta'$  decays for  $\phi = 39.3^\circ$ ,  $\omega_b = 0.36$  GeV (dashed curve), 0.40 GeV (solid curve), and 0.44 GeV (dotted curve).

$$\lambda_{CP} = \frac{V_{tb}^* V_{td} \langle f | H_{\text{eff}} | \bar{B}^0 \rangle}{V_{tb} V_{td}^* \langle f | H_{\text{eff}} | B^0 \rangle} = e^{2i\alpha} \frac{1 + ze^{i(\delta-\alpha)}}{1 + ze^{i(\delta+\alpha)}}. \quad (71)$$

Here the ratio  $z$  and the strong phase  $\delta$  have been defined previously. In pQCD approach, since both  $z$  and  $\delta$  are calculable, it is easy to find the numerical values of  $\mathcal{A}_{CP}^{\text{dir}}$  and  $\mathcal{A}_{CP}^{\text{mix}}$  for the considered decay processes.

By using the central values of the input parameters, one found the pQCD predictions (in unit of  $10^{-2}$ ) for the direct and mixing-induced  $CP$ -violating asymmetries of the considered decays

$$\begin{aligned} \mathcal{A}_{CP}^{\text{dir}}(B^0 \rightarrow \omega \eta) &= -69.1_{-13.4}^{+15.1}(\alpha), \\ \mathcal{A}_{CP}^{\text{mix}}(B^0 \rightarrow \omega \eta) &= +66.9_{-15.8}^{+5.3}(\alpha), \end{aligned} \quad (72)$$

$$\begin{aligned} \mathcal{A}_{CP}^{\text{dir}}(B^0 \rightarrow \omega \eta') &= +13.9_{-3.5}^{+4.1}(\alpha), \\ \mathcal{A}_{CP}^{\text{mix}}(B^0 \rightarrow \omega \eta') &= +65.8_{-55.2}^{+29.1}(\alpha), \end{aligned} \quad (73)$$

where the dominant errors come from the variations of  $\alpha = 100^\circ \pm 20^\circ$ .

In Fig. 4, we show the  $\alpha$ -dependence of the pQCD predictions for the direct and the mixing-induced  $CP$ -violating asymmetry for the  $B^0 \rightarrow \omega \eta$  (solid curve) and  $B^0 \rightarrow \omega \eta'$  (dotted curve) decay, respectively. The pQCD predictions in Eqs. (72) and (73) are consistent with the QCDF predictions due to very large uncertainties in the QCDF approach [1].

If we integrate the time variable  $t$ , we will get the total  $CP$  asymmetry for  $B^0 \rightarrow \omega \eta^{(\prime)}$  decays (in units of  $10^{-2}$ ):

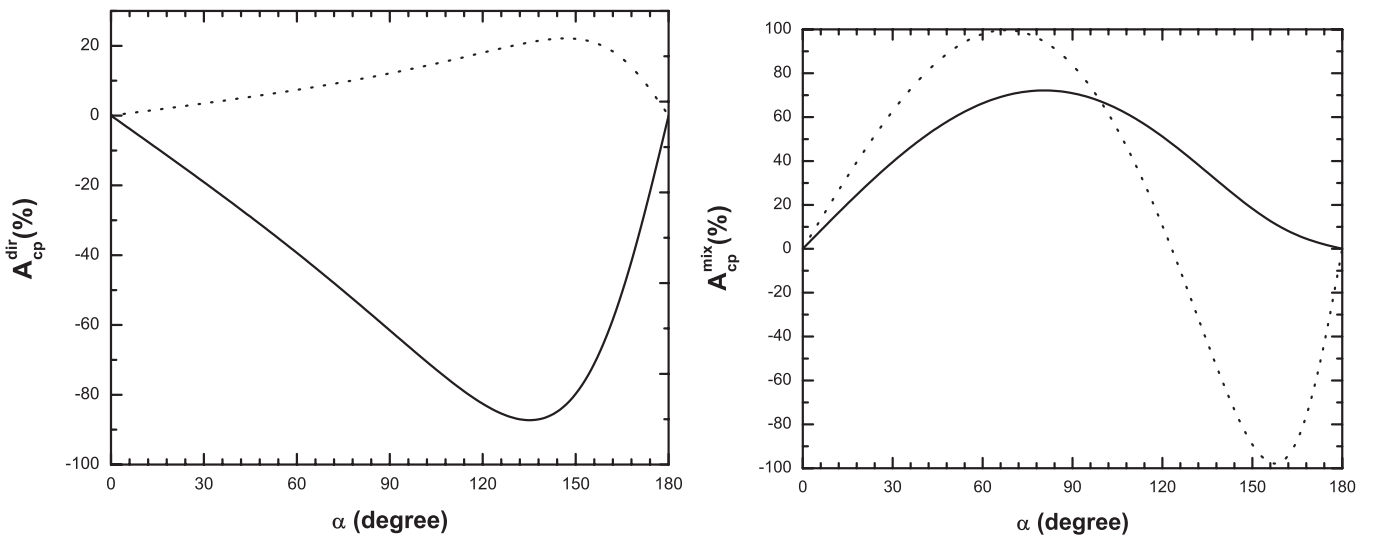


FIG. 4. The direct and mixing-induced  $CP$  asymmetry (in percentage) of the  $B^0 \rightarrow \omega \eta$  (solid curve) and  $\omega \eta'$  (dotted curve) decay as a function of the CKM angle  $\alpha$ .

$$\mathcal{A}_{CP}^{\text{tot}}(B^0 \rightarrow \omega \eta) = -11_{-15.1}^{+12.1}(\alpha), \quad (74)$$

$$\mathcal{A}_{CP}^{\text{tot}}(B^0 \rightarrow \omega \eta') = +40.6_{-24.2}^{+11.8}(\alpha). \quad (75)$$

For the  $B^0 \rightarrow \phi \eta^{(\prime)}$  decay modes, however, there is no  $CP$  asymmetry, the reason is that they involve only penguin contributions and one type of CKM elements.

It is worth mentioning that although the  $CP$ -violating asymmetries of  $B \rightarrow \omega \eta^{(\prime)}$  decays are rather large in size, it may be difficult to measure them because of the predicted small branching ratios at the  $10^{-7}$  level [33].

#### D. Effects of the possible gluonic component of $\eta'$

Up to now, we have not considered the possible contributions to the branching ratios and  $CP$ -violating asymmetries of  $B \rightarrow \omega(\phi)\eta^{(\prime)}$  decays induced by the possible gluonic component of the  $\eta$  and  $\eta'$  meson. For the  $\eta$  meson, one generally believes that its gluonic component is negligibly small. For the  $\eta'$  meson, however, a large gluonic component is generally expected because of the observed very large  $B \rightarrow K \eta'$  branching ratio.

When a nonzero gluonic component exists in the  $\eta'$  meson, an additional decay amplitude  $\mathcal{M}'$  will be produced. Such a decay amplitude may construct or destruct with the ones from the  $q\bar{q}$  ( $q = u, d, s$ ) components of  $\eta'$ , the branching ratios of the decays in question may be increased or decreased accordingly.

In Ref. [9], by employing the pQCD factorization approach, Charng, Kurimoto, and Li calculated the flavor-singlet contribution to the  $B \rightarrow \eta^{(\prime)}$  transition form factors induced by the Feynman diagrams with the two gluons emitted from the light quark of the  $B$  meson (see Fig. 1 of Ref. [9]), the dominant gluonic contribution is negligible for the  $B \rightarrow \eta$  form factor, and also small (less than 5%) for the  $B \rightarrow \eta'$  ones [13].

Following the procedure of Ref. [9] and using the formulae given there, we also calculate the gluonic contributions to  $B \rightarrow \omega(\phi)\eta'$  decays. If we add the gluonic contribution to the form factor  $F_0^{B \rightarrow \eta'}$  but keep all other inputs in their default central values, we find numerically that

$$\text{Br}(B^0 \rightarrow \omega \eta') = 0.82 \times 10^{-7}, \quad (76)$$

$$\text{Br}(B^0 \rightarrow \phi \eta') = 6.5 \times 10^{-9}. \quad (77)$$

One can see that the variation of the central values of the pQCD predictions induced by the inclusion of the gluonic contribution is only about  $\pm 10\%$ , much smaller than the theoretical uncertainties from the variations of input parameters  $\omega_b$ ,  $m_s$ , or  $\alpha$ .

#### V. SUMMARY

In this paper, we calculated the branching ratios of  $B^0 \rightarrow \omega \eta^{(\prime)}$ ,  $\phi \eta^{(\prime)}$  decays and  $CP$ -violating asymmetries of

$B^0 \rightarrow \omega \eta^{(\prime)}$  decays at the leading order by using the pQCD factorization approach.

Besides the usual factorizable diagrams, the nonfactorizable and annihilation diagrams are also calculated analytically. Although the nonfactorizable and annihilation contributions are subleading for the branching ratios of the considered decays, they are not negligible. Furthermore these diagrams provide the necessary strong phase required by a nonzero  $CP$ -violating asymmetry for the considered decays.

After calculating all the diagrams, we found the branching ratios of the four related decays are very small,  $\text{Br}(B \rightarrow \omega \eta^{(\prime)})$  are at the order of  $O(10^{-7})$  and  $\text{Br}(B \rightarrow \phi \eta^{(\prime)})$  are around  $10^{-9}$ . We also predict the direct and mixing-induced  $CP$  asymmetries of the  $B \rightarrow \omega \eta^{(\prime)}$ . Moreover, we compare our results with the current experimental data and the theoretical predictions in the QCDF approach. In short, we found that

- (i) For the  $CP$ -averaged branching ratios of the considered decay modes, the pQCD predictions are

$$\text{Br}(B^0 \rightarrow \omega \eta) = (2.7_{-1.0}^{+1.1}) \times 10^{-7}, \quad (78)$$

$$\text{Br}(B^0 \rightarrow \omega \eta') = (0.75_{-0.33}^{+0.37}) \times 10^{-7}, \quad (79)$$

$$\text{Br}(B^0 \rightarrow \phi \eta) = (6.3_{-1.9}^{+3.3}) \times 10^{-9}, \quad (80)$$

$$\text{Br}(B^0 \rightarrow \phi \eta') = (7.3_{-2.6}^{+3.5}) \times 10^{-9}, \quad (81)$$

where the various errors as specified in Eqs. (62)–(65) have been added in quadrature. The inclusion of the gluonic contribution can change the branching ratios of ( $B \rightarrow \omega \eta'$ ,  $\phi \eta'$ ) decays by about 10% in magnitude.

- (ii) The pQCD predictions for the  $CP$ -violating asymmetries of  $B \rightarrow \omega \eta^{(\prime)}$  decays are large in size.
- (iii) The major theoretical errors are induced by the uncertainties of the input parameters  $\omega_B$ , the mass  $m_s$ , the CKM angle  $\alpha$ , and the Gegenbauer moment  $a_2^{\eta_{q(s)}}$ .

#### ACKNOWLEDGMENTS

We are very grateful to Cai-Dian Lü, Ying Li, Xin Liu, and Huisheng Wang for helpful discussions. This work is partly supported by the National Natural Science Foundation of China under Grant No. 10575052, and by the Specialized Research Fund for the doctoral Program of higher education (SRFDP) under Grant No. 20050319008.

#### APPENDIX: RELATED FUNCTIONS

We show here the function  $h_i$  appearing in the expressions of the decay amplitudes in Sec. III, coming from the Fourier transformations of the function  $H^{(0)}$ ,

$$h_e(x_1, x_3, b_1, b_3) = K_0(\sqrt{x_1 x_3} m_B b_1) [\theta(b_1 - b_3) K_0(\sqrt{x_3} m_B b_1) I_0(\sqrt{x_3} m_B b_3) + \theta(b_3 - b_1) K_0(\sqrt{x_3} m_B b_3) I_0(\sqrt{x_3} m_B b_1)] S_t(x_3), \quad (\text{A1})$$

$$h_a(x_2, x_3, b_2, b_3) = K_0(i\sqrt{x_2 x_3} m_B b_2) [\theta(b_3 - b_2) K_0(i\sqrt{x_3} m_B b_3) I_0(i\sqrt{x_3} m_B b_2) + \theta(b_2 - b_3) K_0(i\sqrt{x_3} m_B b_2) I_0(i\sqrt{x_3} m_B b_3)] S_t(x_3), \quad (\text{A2})$$

$$h_f(x_1, x_2, x_3, b_1, b_2) = \{\theta(b_2 - b_1) I_0(M_B \sqrt{x_1 x_3} b_1) K_0(M_B \sqrt{x_1 x_3} b_2) + (b_1 \leftrightarrow b_2)\} \begin{cases} K_0(M_B F_{(1)} b_2), & \text{for } F_{(1)}^2 > 0 \\ \frac{\pi i}{2} H_0^{(1)}(M_B \sqrt{|F_{(1)}^2|} b_2), & \text{for } F_{(1)}^2 < 0 \end{cases}, \quad (\text{A3})$$

$$h_g^2(x_1, x_2, x_3, b_1, b_2) = \{\theta(b_1 - b_2) K_0(i\sqrt{x_2 x_3} b_1 M_B) I_0(i\sqrt{x_2 x_3} b_2 M_B) + (b_1 \leftrightarrow b_2)\} K_0(\sqrt{x_1 + x_2 + x_3 - x_1 x_3 - x_2 x_3} b_1 M_B), \quad (\text{A4})$$

$$h_f^4(x_1, x_2, x_3, b_1, b_2) = \{\theta(b_1 - b_2) K_0(i\sqrt{x_2 x_3} b_1 M_B) I_0(i\sqrt{x_2 x_3} b_2 M_B) + (b_1 \leftrightarrow b_2)\} \begin{cases} K_0(M_B F_{(2)} b_1), & \text{for } F_{(2)}^2 > 0 \\ \frac{\pi i}{2} H_0^{(1)}(M_B \sqrt{|F_{(2)}^2|} b_1), & \text{for } F_{(2)}^2 < 0 \end{cases}, \quad (\text{A5})$$

where  $J_0$  is the Bessel function,  $K_0$  and  $I_0$  are the modified Bessel functions  $K_0(-ix) = -(\pi/2)Y_0(x) + i(\pi/2)J_0(x)$ ,  $H_0^{(1)}(z) = J_0(z) + iY_0(z)$ , and the  $F_{(j)}$  are defined by

$$F_{(1)}^2 = (x_1 - x_2)x_3, \quad (\text{A6})$$

$$F_{(2)}^2 = (x_1 - x_2)x_3. \quad (\text{A7})$$

The threshold resummation form factor  $S_t(x_i)$  is adopted from Ref. [24]

$$S_t(x) = \frac{2^{1+2c} \Gamma(3/2 + c)}{\sqrt{\pi} \Gamma(1 + c)} [x(1-x)]^c, \quad (\text{A8})$$

where the parameter  $c = 0.3$ . This function is normalized to unity.

The Sudakov factors appearing in Sec. III are defined as

$$S_{ab}(t) = s(x_1 m_B / \sqrt{2}, b_1) + s(x_3 m_B / \sqrt{2}, b_3) + s((1 - x_3) m_B / \sqrt{2}, b_3) - \frac{1}{\beta_1} \left[ \ln \frac{\ln(t/\Lambda)}{-\ln(b_1 \Lambda)} + \ln \frac{\ln(t/\Lambda)}{-\ln(b_3 \Lambda)} \right], \quad (\text{A9})$$

$$S_{cd}(t) = s(x_1 m_B / \sqrt{2}, b_1) + s(x_2 m_B / \sqrt{2}, b_2) + s((1 - x_2) m_B / \sqrt{2}, b_2) + s(x_3 m_B / \sqrt{2}, b_1) + s((1 - x_3) m_B / \sqrt{2}, b_1) - \frac{1}{\beta_1} \left[ 2 \ln \frac{\ln(t/\Lambda)}{-\ln(b_1 \Lambda)} + \ln \frac{\ln(t/\Lambda)}{-\ln(b_2 \Lambda)} \right], \quad (\text{A10})$$

$$S_{ef}(t) = s(x_1 m_B / \sqrt{2}, b_1) + s(x_2 m_B / \sqrt{2}, b_2) + s((1 - x_2) m_B / \sqrt{2}, b_2) + s(x_3 m_B / \sqrt{2}, b_2) + s((1 - x_3) m_B / \sqrt{2}, b_2) - \frac{1}{\beta_1} \left[ \ln \frac{\ln(t/\Lambda)}{-\ln(b_1 \Lambda)} + 2 \ln \frac{\ln(t/\Lambda)}{-\ln(b_2 \Lambda)} \right], \quad (\text{A11})$$

$$S_{gh}(t) = s(x_2 m_B / \sqrt{2}, b_2) + s(x_3 m_B / \sqrt{2}, b_3) + s((1 - x_2) m_B / \sqrt{2}, b_2) + s((1 - x_3) m_B / \sqrt{2}, b_3) - \frac{1}{\beta_1} \left[ \ln \frac{\ln(t/\Lambda)}{-\ln(b_2 \Lambda)} + \ln \frac{\ln(t/\Lambda)}{-\ln(b_3 \Lambda)} \right], \quad (\text{A12})$$

where the function  $s(q, b)$  is defined in the Appendix A of Ref. [19]. The scale  $t_i$ 's in the above equations are chosen as

$$\begin{aligned}
t_e^1 &= \max(\sqrt{x_3}m_B, 1/b_1, 1/b_3), \\
t_e^2 &= \max(\sqrt{x_1}m_B, 1/b_1, 1/b_3), \\
t_e^3 &= \max(\sqrt{x_3}m_B, 1/b_2, 1/b_3), \\
t_e^4 &= \max(\sqrt{x_2}m_B, 1/b_2, 1/b_3), \\
t_f &= \max(\sqrt{x_1x_3}m_B, \sqrt{(x_1 - x_2)x_3}m_B, 1/b_1, 1/b_2), \\
t_f^3 &= \max(\sqrt{x_1 + x_2 + x_3 - x_1x_3 - x_2x_3}m_B, \\
&\quad \sqrt{x_2x_3}m_B, 1/b_1, 1/b_2), \\
t_f^4 &= \max(\sqrt{x_2x_3}m_B, \sqrt{(x_1 - x_2)x_3}m_B, 1/b_1, 1/b_2). \quad (\text{A13})
\end{aligned}$$

They are given as the maximum energy scale appearing in each diagram to kill the large logarithmic radiative corrections.

- 
- [1] M. Beneke and M. Neubert, Nucl. Phys. **B675**, 333 (2003); **B651**, 225 (2003).
- [2] M. Beneke, G. Buchalla, M. Neubert, and C. T. Sachrajda, Phys. Rev. Lett. **83**, 1914 (1999).
- [3] H. N. Li and H. L. Yu, Phys. Rev. Lett. **74**, 4388 (1995); Phys. Lett. B **353**, 301 (1995); Phys. Rev. D **53**, 2480 (1996); Y. Y. Keum, H. N. Li, and A. I. Sanda, Phys. Rev. D **63**, 054008 (2001).
- [4] E. Kou and A. I. Sanda, Phys. Lett. B **525**, 240 (2002).
- [5] X. Liu, H. S. Wang, Z. J. Xiao, L. B. Guo, and C. D. Lü, Phys. Rev. D **73**, 074002 (2006).
- [6] H. S. Wang, X. Liu, Z. J. Xiao, L. B. Guo, and C. D. Lü, Nucl. Phys. **B738**, 243 (2006).
- [7] Z. J. Xiao, D. Q. Guo, and X. F. Chen, Phys. Rev. D **75**, 014018 (2007).
- [8] Z. J. Xiao, Xin Liu, and H. S. Wang, Phys. Rev. D **75**, 034017 (2007); Z. J. Xiao, X. F. Chen, and D. Q. Guo, hep-ph/0608222 [Eur. Phys. J. C (to be published)]; X. F. Chen, D. Q. Guo, and Z. J. Xiao, hep-ph/0701146.
- [9] Y. Y. Charng, T. Kurimoto, and H. N. Li, Phys. Rev. D **74**, 074024 (2006).
- [10] E. Barberio *et al.* (Heavy Flavor Averaging Group), hep-ex/0603003, updated in <http://www.slac.stanford.edu/xorg/hfag>.
- [11] J. Schümann *et al.* (Belle Collaboration), hep-ex/0701046.
- [12] A. Ali and A. Ya. Parkhomenko, Eur. Phys. J. C **30**, 183 (2003).
- [13] H. N. Li, Report Nanjing Normal University, People's Republic of China, 2006.
- [14] C.-H. V. Chang and H. N. Li, Phys. Rev. D **55**, 5577 (1997); T.-W. Yeh and H. N. Li, Phys. Rev. D **56**, 1615 (1997); H. N. Li, Prog. Part. Nucl. Phys. **51**, 85 (2003), and reference therein.
- [15] G. P. Lepage and S. J. Brodsky, Phys. Rev. D **22**, 2157 (1980).
- [16] S. Descotes-Genon and C. T. Sachrajda, Nucl. Phys. **B625**, 239 (2002); Z. T. Wei and M. Z. Yang, Nucl. Phys. **B642**, 263 (2002); M. Beneke and T. Feldmann, Nucl. Phys. **B685**, 249 (2004).
- [17] H. N. Li and B. Tseng, Phys. Rev. D **57**, 443 (1998).
- [18] For a review see G. Buchalla, A. J. Buras, and M. E. Lautenbacher, Rev. Mod. Phys. **68**, 1125 (1996).
- [19] C. D. Lü, K. Ukai, and M. Z. Yang, Phys. Rev. D **63**, 074009 (2001).
- [20] W.-M. Yao *et al.* (Particle Data Group), J. Phys. G **33**, 1 (2006).
- [21] T. Feldmann, P. Kroll, and B. Stech, Phys. Rev. D **58**, 114006 (1998); Phys. Lett. B **449**, 339 (1999); T. Feldmann, Int. J. Mod. Phys. A **15**, 159 (2000).
- [22] R. Escribano and J. M. Frere, J. High Energy Phys. 06 (2005) 029; J. Schechter, A. Subbaraman, and H. Weigel, Phys. Rev. D **48**, 339 (1993).
- [23] E. Kou, Phys. Rev. D **63**, 054027 (2001).
- [24] T. Kurimoto, H. N. Li, and A. I. Sanda, Phys. Rev. D **65**, 014007 (2001).
- [25] C. D. Lü and M. Z. Yang, Eur. Phys. J. C **28**, 515 (2003).
- [26] P. Ball, J. High Energy Phys. 09 (1998) 005; 01 (1999) 010.
- [27] P. Ball and R. Zwicky, Phys. Rev. D **71**, 014015 (2005).
- [28] P. Ball, V. M. Braun, and A. Lenz, J. High Energy Phys. 05 (2006) 004.
- [29] P. Ball, V. M. Braun, Y. Koike, and K. Tanaka, Nucl. Phys. **B529**, 323 (1998).
- [30] H. W. Huang, C. D. Lü, T. Morii, Y. L. Shen, G. L. Song, and J. Zhu, Phys. Rev. D **73**, 014011 (2006).
- [31] Y. Li and C. D. Lü, Phys. Rev. D **73**, 014024 (2006).
- [32] P. Ball and R. Zwicky, Phys. Rev. D **71**, 014029 (2005).
- [33] P. Ball *et al.*, in Standard model physics (and more) at the LHC, Geneva, 1999, CERN-TH-2000-101, 2000, p. 305; hep-ph/0003238; T. Skwarnicki, Aspen 2007, Aspen, Colorado (unpublished).